



Statistical Analysis of Hydrodynamic Forces in Power-Law Fluid Flow in a Channel: Circular Versus Semi-Circular Cylinder

Rashid Mahmood¹, Afraz Hussain Majeed¹, Muhammad Tahir², Imran Saddique^{3*}, Nawaf N. Hamadneh^{4*}, Ilyas Khan⁵ and Asif Mehmood¹

¹Department of Mathematics, Air University, Islamabad, Pakistan, ²College of Computing and Informatics, Saudi Electronic University, Riyadh, Saudi Arabia, ³Department of Mathematics, University of Management and Technology, Lahore, Pakistan, ⁴Department of Basic Sciences, College of Science and Theoretical Studies, Saudi Electronic University, Riyadh, Saudi Arabia, ⁵Department of Mathematics, College of Science Al-Zulfi, Majmaah University, Al-Majmaah, Saudi Arabia

OPEN ACCESS

Edited by:

Jordan Yankov Hristov,
University of Chemical Technology
and Metallurgy, Bulgaria

Reviewed by:

Marin I. Marin,
Transilvania University of Braşov,
Romania
Muhammad Mubashir Bhatti,
Shandong University of Science and
Technology, China

*Correspondence:

Nawaf N. Hamadneh
nwwaf977@gmail.com
Imran Saddique
imransmsrazi@gmail.com

Specialty section:

This article was submitted to
Mathematical and Statistical Physics,
a section of the journal
Frontiers in Physics

Received: 07 December 2021

Accepted: 13 January 2022

Published: 21 March 2022

Citation:

Mahmood R, Majeed AH, Tahir M, Saddique I, Hamadneh NN, Khan I and Mehmood A (2022) Statistical Analysis of Hydrodynamic Forces in Power-Law Fluid Flow in a Channel: Circular Versus Semi-Circular Cylinder. *Front. Phys.* 10:830408. doi: 10.3389/fphy.2022.830408

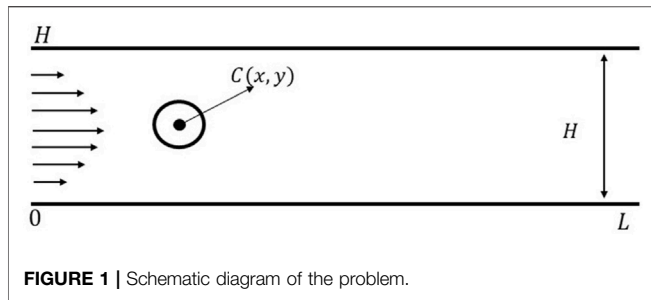
This numerical study is about the steady incompressible non-Newtonian fluid flow in a channel with static obstacles. The flow field is governed by the Generalized Navier-Stokes equations incorporating the constitutive relation of power-law fluids. Three cases are considered: 1) circular obstacle (C_1), 2) semicircular obstacle (C_2), and 3) both circular and semicircular obstacles. A range of values of the power-law index $0.3 \leq n \leq 1.7$ are considered at $Re = 20$ to check the impact of shear-thinning and shear-thickening viscosity on the drag and lift coefficients. The correlation between drag and lift coefficients is calculated against the power-law index. The simulated results of velocity and pressure are investigated at different sections of the channel. Benchmark results of drag and lift for the Newtonian fluid are reproduced as a special case. A strong positive correlation is observed between drag and lift coefficients in the case of a single obstacle, while in the case of dual obstacles and inverse correlation, drag and lift coefficients have been found.

Keywords: power-law fluid, circular cylinder, parabolic flow, fluid forces, FEM computation, correlation

INTRODUCTION

The fluid flow past solid bodies is one of the practical problems being investigated in the domain of fluid mechanics, and hence, it has attained the focus of engineers and scientists. The phenomenon has a lot of engineering and industrial applications. In the past, a lot of work has been done, and many aspects of flow have been investigated for Newtonian fluid both in experimental and numerical ways [1–7]. The investigation of flow around rigid bodies has many engineering applications such as the aerodynamics of chimney stacks, skyscrapers, suspension bridges, etc. During the last decade, the fluid past the bluff bodies of different shapes and sizes has been investigated by many researchers [8–10]. The wake produced by the separation of fluid past the bluff bodies mainly depends on the shape and size of the obstacles [11–15]. To investigate the steady and periodic wake, the effective Reynolds number is used by Dumouchel et al. [16]. The effect of different Reynolds numbers on fluid flow past non-spherical bodies was observed by Berrone [17], Liu and Kopp [18], and Schewe [19].

The medical and engineering contribution of viscous fluid has been truly recognized for the last couple of centuries. Engineers and medical scientists paid special attention to understanding the



nature of fluids and more specifically to the visible fluids. As science evolved, the types of fluids, the flow characteristics, and the invisible forces involved in fluid flow are the major discoveries that are being used nowadays for the benefit of mankind. In recent times, flow geometry is one of the main focuses of attention for many researchers. Understanding the elastic and plastic characteristics of some fluids is due to such attention. The fluid flow is mainly dependent on certain factors like pressure, velocity, and viscosity. Mathematically speaking, the shear stress and shear rate of strain are the key factors to be investigated together with viscosity [20–24].

Based on generalized Newtonian fluids, this work is related to the fluid flow around the obstacles of circular and semicircular shape. The flow regime is compared for both cases. For different values of Reynolds numbers, the Newtonian fluid flow around obstacles of different shapes has been investigated by many [25,26]. The laminar flow characteristics can be observed for

low values of Reynold numbers, generally for Newtonian fluids. The fluids with shear-thinning viscosity are considered the simplest version of non-Newtonian fluids, but with the advancement of computational techniques, the fluids with shear-thickening viscosity are attaining the interest of researchers [27]. For many non-Newtonian fluids, the shearing characteristics are investigated in reference [28].

Recognizing the industrial applications of flow around semi-cylinders, this work is confined to some numerical results. The comparison is made with the results of the circular cylinder. We organize the manuscript as follows. **Section 2** is concerned with the mathematical modeling and numerical approach for this work. **Section 3** displays the results and discussion for the involved factors. The conclusion of the present study is revealed in **Section 4**.

MATHEMATICAL MODELING AND NUMERICAL SCHEME

The Navier Stokes equations provide the way to understand and deal with fluid engineering [29–33]. These equations are set on nonlinear partial differential equations, due to which analytical solution of such problems as well as of other problems arising as models of wave propagation [34,35] is often difficult. In order to solve them, one needs to approach a numerical solution. Among many numerical tools reported in the literature to deal with the mechanics of fluid flow, the finite element method (FEM) is the prominent one. The functionality of the finite element method

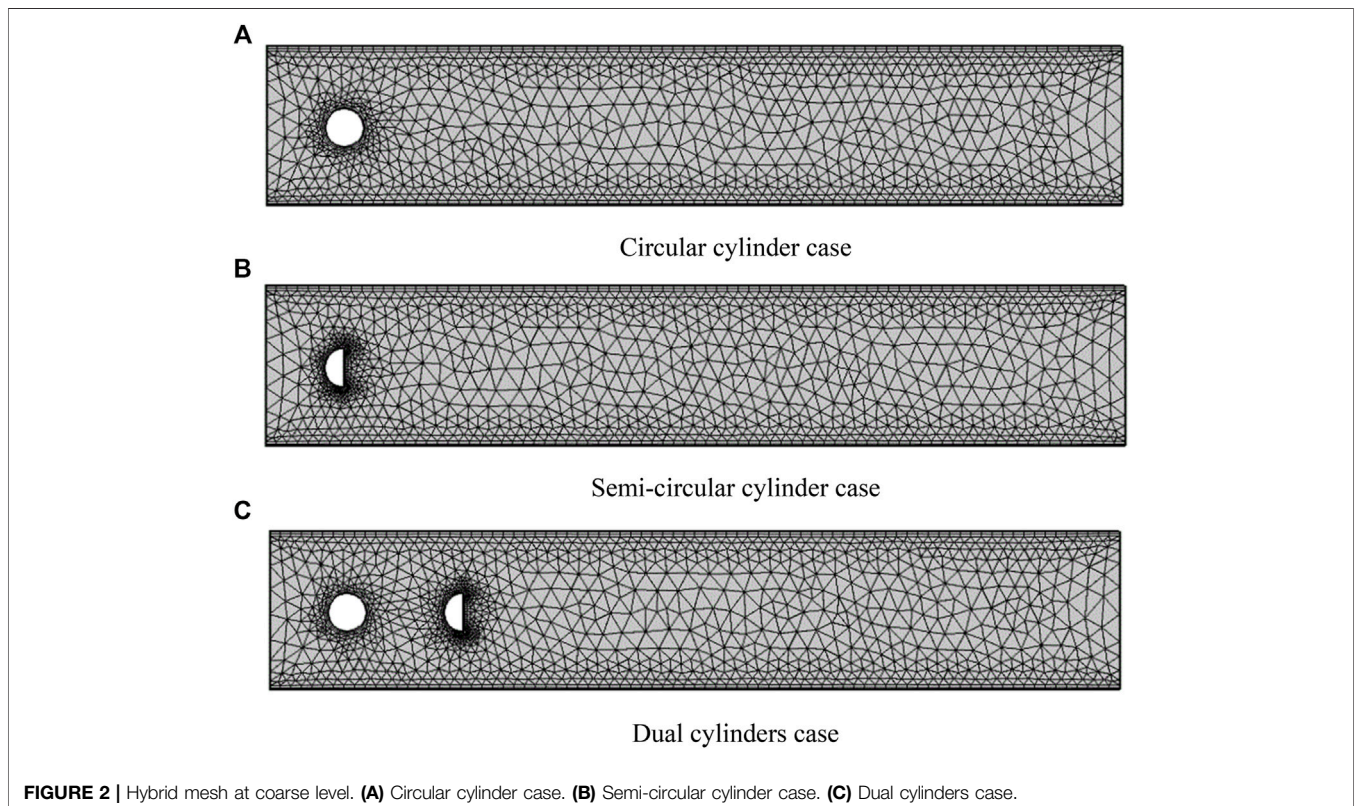


TABLE 1 | Impacts of n on drag and lift coefficients for single obstacles.

n	Circular cylinder		Semi-cylinder	
	C_D	C_L	C_D	C_L
0.3	2.285,163	-0.01598	2.621,777	-0.01572
0.5	3.022671	-0.01433	3.311,908	-0.01482
0.7	3.919,195	-0.00904	4.134,044	-0.01232
1.0	5.578,019	0.010645	5.646,302	-0.00185
1.3	7.736,785	0.060306	7.589,954	0.025846
1.5	9.672,510	0.132,124	9.286,573	0.064137
1.7	12.16879	0.256,646	11.45529	0.131,802

and the mathematical modeling for our problem is described in references [36–42].

$$\nabla \cdot \mathbf{u} = 0 \tag{1}$$

$$\rho(\mathbf{u} \cdot \nabla \mathbf{u}) = -\nabla p + \nabla \cdot \boldsymbol{\tau}, \tag{2}$$

where the symbols have their usual meanings.

Power-Law Fluid

The power-law fluid was first suggested by W. Ostwald in 1925. Although the simplest model shows dependence upon the shear rate with the minimal number of parameters, it is representative of many non-Newtonian fluids. One of the advantages of this model is that it gives rise to analytical solutions in many cases, and hence, this model is widely used in applications. The model [25] is given by the following:

$$\tau = m(\dot{\gamma})^n, \tag{3}$$

where τ and $\dot{\gamma}$ are the shear stress and shear rate while n and m are the power-law index and consistency index, respectively.

Flow Configuration

A circular cylinder with a diameter $D = 0.1$ is placed in a channel at various positions. The dimension of the given domain is $[0, 2.2] \times [0, 0.41]$. The circular obstacle C_1 and semi-circular C_2 are fixed at $(0.2, 0.2)$ in the channel for two different studies. Later, C_1 and C_2 are placed in the channel simultaneously in a series at $(0.2, 0.2)$ and $(0.5, 0.2)$, respectively. The flow analysis is two-dimensional as there is no flow in the z -direction. The x -directional inlet is set at the left-hand side of the channel. An inflow profile is parabolic with maximum velocity $u_{\max} = 0.3$ at the inlet of the channel. The y -direction explains the fully developed x -directional flow profile. A do-nothing boundary

TABLE 2 | Impacts of n on drag and lift coefficients for dual obstacles.

n	C_D Dual cylinders		C_L Dual cylinders	
	C_1	C_2	C_1	C_2
0.3	2.238,806	0.628,784	-0.01286	0.048534
0.5	2.941,278	1.189,861	-0.01046	0.045178
0.7	3.811,935	1.853,629	-0.00488	0.048908
1.0	5.443,447	3.242,317	0.014348	0.057837
1.3	7.578,352	5.417,577	0.061964	0.056739
1.5	9.494,071	7.431,205	0.131,950	0.040403
1.7	11.96733	9.94492	0.255,813	0.029470

TABLE 3 | Correlation coefficient for C_D and C_L (single cylinder).

	Circular	Semi-circular
Correlation coefficient (r)	0.955	0.952

condition at the outlet is chosen. The other walls of the channel are set with no-slip conditions.

As the fluid interacts with the bluff body, the flow pressure exerts some forces on the surface of the cylinder(s) which are quantified as drag and lift. The dimensionless coefficients of these forces are as follows:

$$C_D = \frac{2F_d}{\rho U_{\text{mean}}^2 D}, \tag{4}$$

$$C_L = \frac{2F_l}{\rho U_{\text{mean}}^2 D}. \tag{5}$$

Here, the average velocity is U_{mean} and D is the diameter of the obstacle. **Figure 1** shows the schematic diagram of the geometry used for this analysis. **Figure 2** shows the computational grids at refinement level 1 for all three cases. The governing equation is discretized using FEM to approximate the important quantities like velocity and pressure. The reduced equations are solved using Newton’s method. To stop the nonlinear iterative process, we adopt the following criteria:

$$\left| \frac{\psi^{k+1} - \psi^k}{\psi^{k+1}} \right| \leq 10^{-6} \tag{6}$$

here, k displays the number of iterations and ψ denotes a component of the solution. The non-Newtonian power-law fluid is used to investigate the velocity and pressure behavior. For a fixed value of $Re = 20$, the power-law index is used as an input parameter.

RESULTS AND DISCUSSIONS

A) Code Validation

To validate the solution scheme, the results of Schäfer *et al.* [43] are reproduced for the circular cylinder case at $Re = 20$ and $n = 1$, which is the Newtonian case. The close correspondence is observed for the values of drag and lift between the present work and the published work [43], which gives them confidence in solution methodology. The reference values of C_D and C_L as given in reference [43] are as follows:

$$C_D = 5.579535, \\ C_L = 0.010618.$$

B) Correlation of Fluid Forces

In the present case, viscosity is the function of shear rate $\dot{\gamma}$ and the power law exponent (n) which can give rise to different flow

TABLE 4 | Correlation coefficient for C_D and C_L (dual cylinder).

	Circular (upstream)	Semi-circular (downstream)
Correlation coefficient (r)	0.956	-0.611

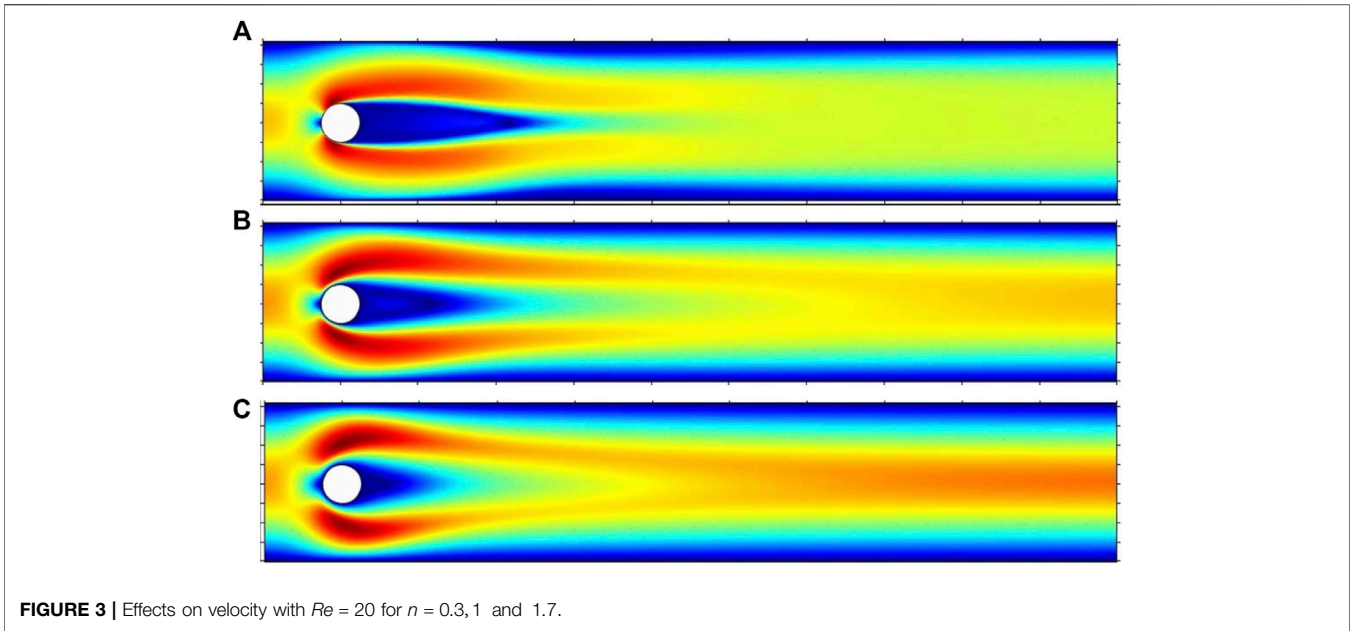


FIGURE 3 | Effects on velocity with $Re = 20$ for $n = 0.3, 1$ and 1.7 .

regimes as shear thinning, Newtonian, and shear thickening. To visualize the influence of n , equidistant values of the n are chosen around the Newtonian case ($n = 1$) for shear thinning and shear thickening behaviors.

Tables (1)-(2) show the results of C_D and C_L calculated for 1) circular cylinder, 2) semi-circular cylinder, and 3) dual cylinder. For a steady flow, the drag is directly related to n . For the shear-thinning case ($n < 1$), the drag is a bit higher at a semi-cylinder than the drag on a circular cylinder. For the shear-thickening case ($n > 1$), the situation is reversed. In the dual cylinder case, less drag is observed than in the single cylinder.

The strength of association between hydrodynamic forces using software SPSS-23 is represented in **Tables (3)-(4)**. A strong and positive correlation is observed between drag and lift when cylinders are taken separately. However, in the case of a dual cylinder placed in a channel, an inverse association between drag and lift is observed at the semi-circular (downstream) cylinder.

C) Impact on Velocity and Pressure

In the present work, the steady, laminar, and incompressible flow is observed using generalized power-law fluid. The

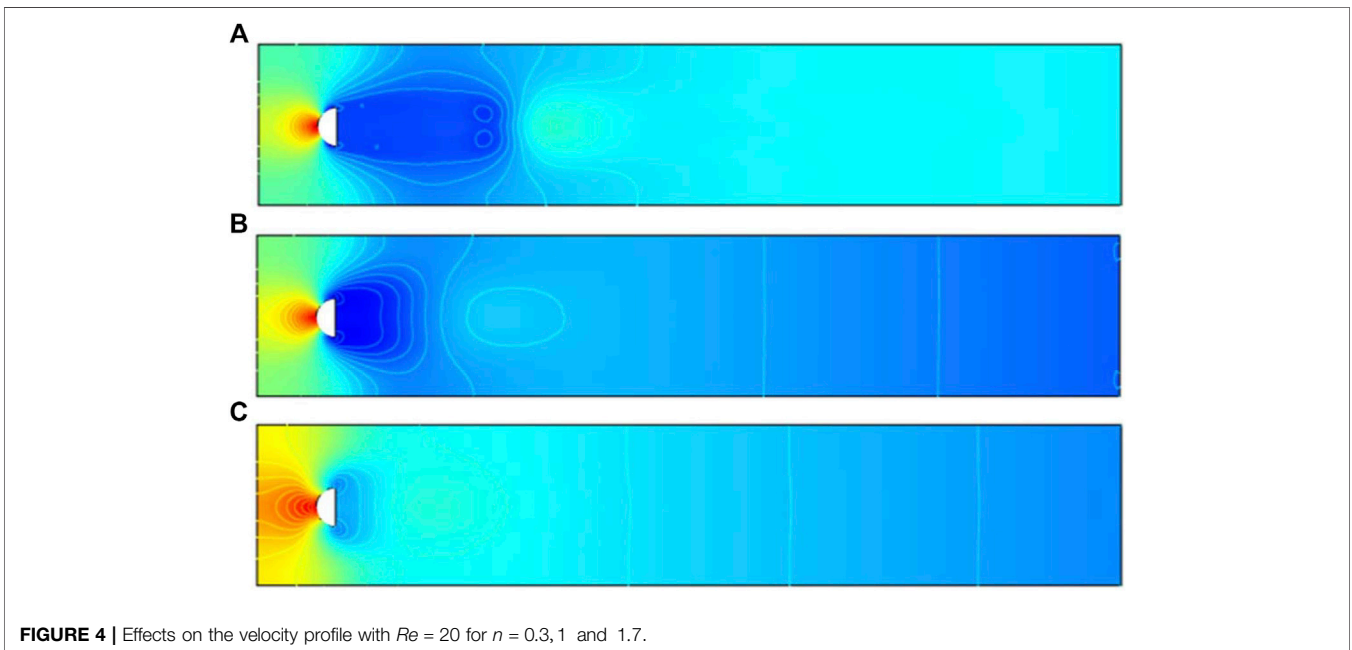


FIGURE 4 | Effects on the velocity profile with $Re = 20$ for $n = 0.3, 1$ and 1.7 .

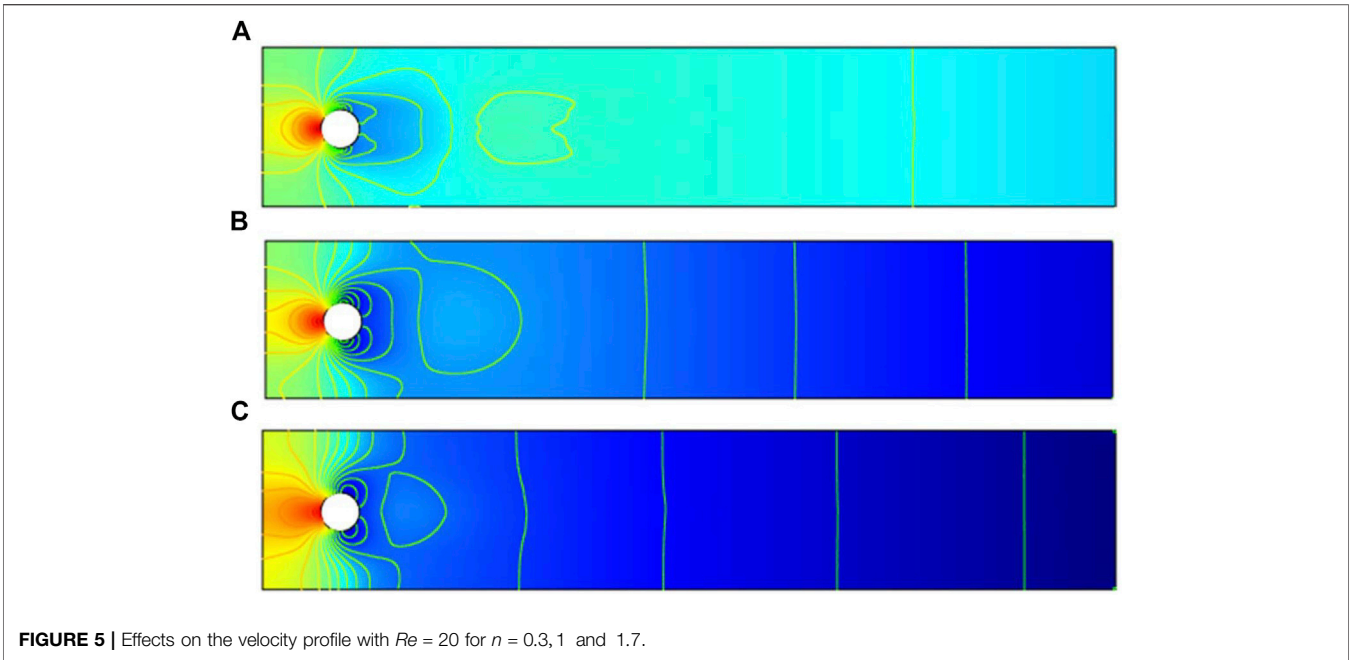


FIGURE 5 | Effects on the velocity profile with $Re = 20$ for $n = 0.3, 1$ and 1.7 .

dimensionless parameter n is used to observe the velocity and pressure behavior for shear-thinning ($n < 1$), shear thickening ($n > 1$), and the Newtonian case ($n = 1$) when the fluid encounters an obstacle. At the stagnation point, the fluid elements come to rest and then accelerate, bifurcating the fluid around the cylinder in the direction of velocity. The maximum velocity is observed at the corner of the cylinder for a specific region. This maximum velocity region around the cylinder increases and moves ahead with the increasing value of n (see

Figures 3, 4, 5). It is also observed that the velocity increases around the central horizontal axis of the channel as fluid thickening increases. As in **Figures 3, 4, 5**, the flow separation is observed in the rear side of the obstacle. The flow separation gets reduced for increasing n . Moreover, in the case of a semi-circular cylinder, the flow separation gets a longer range (see **Figure 4**).

For all three cases, the pressure profiles can be visualized in **Figures 6, 7, 8**. In the free stream region, the pressure gets

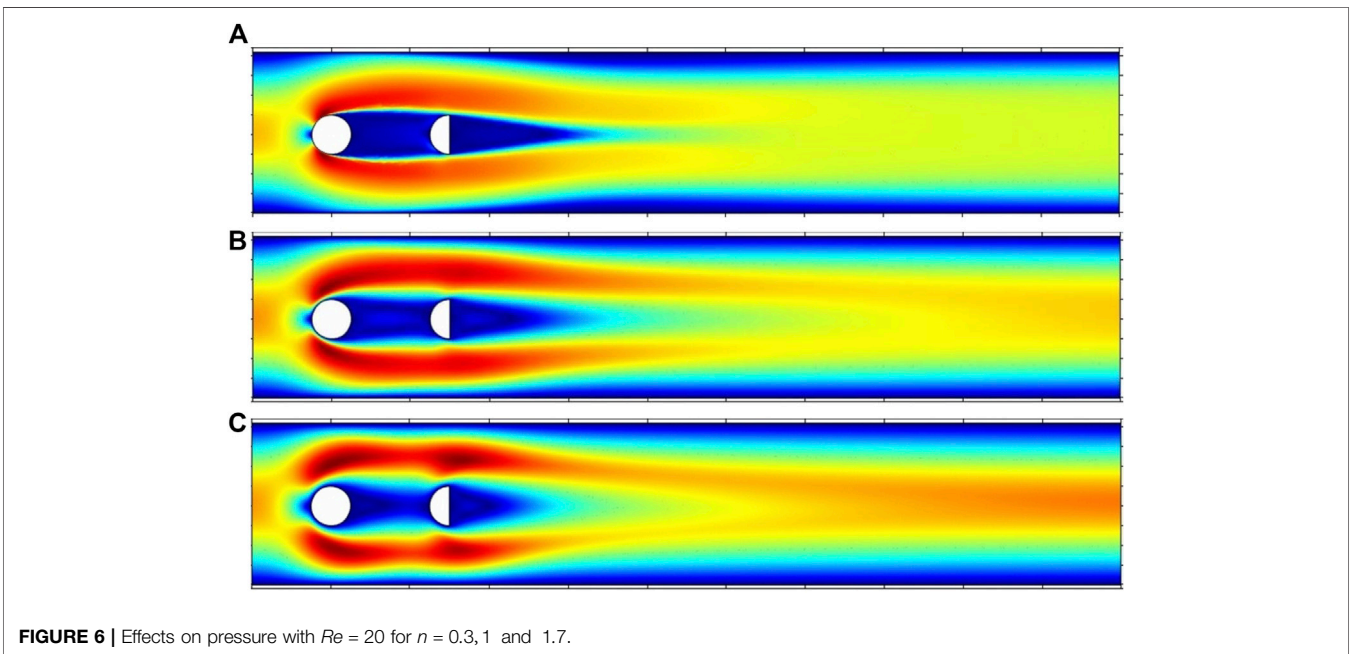


FIGURE 6 | Effects on pressure with $Re = 20$ for $n = 0.3, 1$ and 1.7 .

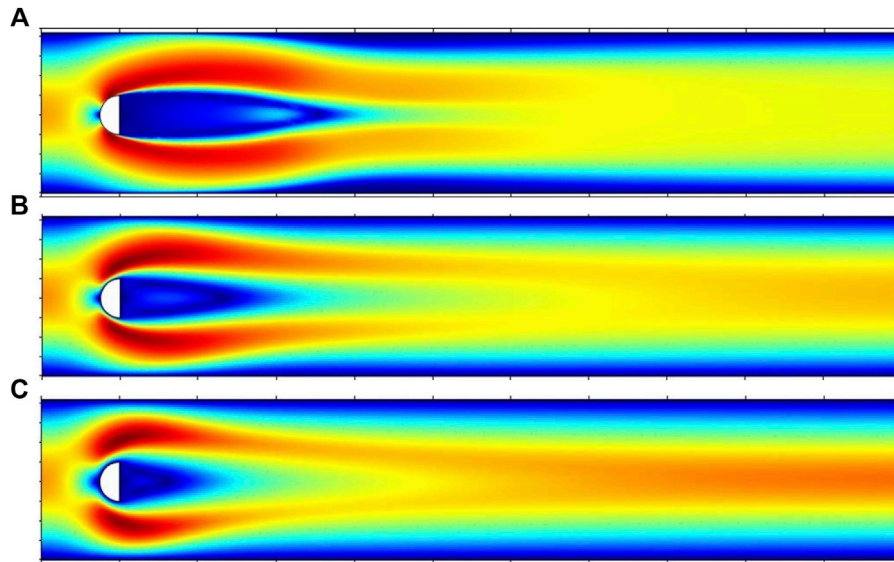


FIGURE 7 | Effects on pressure with $Re = 20$ for $n = 0.3, 1$ and 1.7 .

reduced with increasing n . In the case of the semicircular cylinder (**Figure 7**), an interesting pressure visualization appears for the shear-thinning case ($n = 0.3$). An invisible mild stagnation region appears at around $0.6 \leq x \leq 0.9$, and then it gets evenly distributed afterward. In the dual cylinder case (**Figure 8**), the increasing pressure is observed up to the walls of the channel before the first obstacle (see **Figure 8C**), and the presence of the second obstacle has a significant impact on the pressure spread together with the increasing value of n .

D) Line Graph Behavior

In **Figure 9**, we demonstrate the executed u -velocity at several power-law indexes. In detail, $x = 0.0$ the fluid is initially injected at the inlet of the channel with a parabolic profile. The line graphs of u -velocity are drawn in the free stream region at $x = 1.5$ to observe the impact of the n on velocity. It is observed that shear-thinning fluid moves closer to the channel walls like in the $n = 0.3$ case. The distance of the fluid flow and the channel walls increases with the increasing fluid thickness like $n = 1.7$ in **Figure 9**.

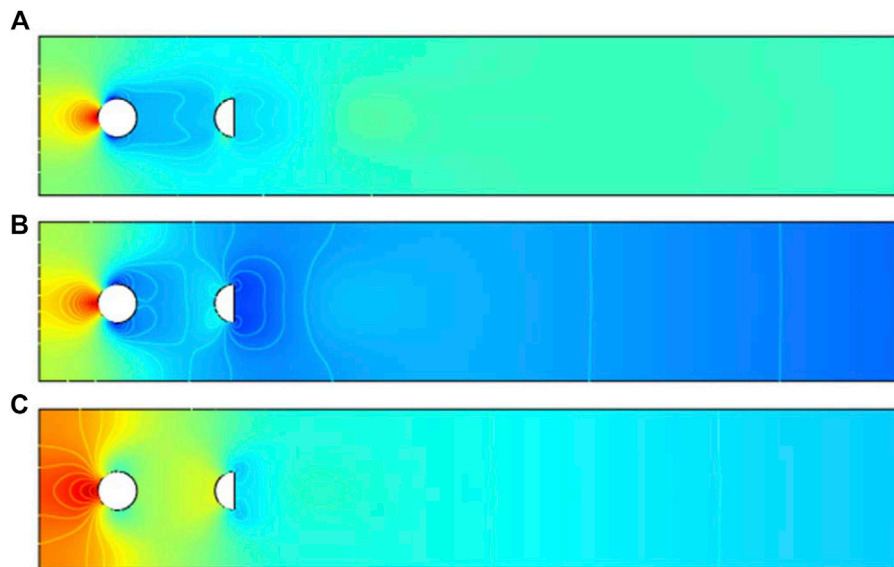


FIGURE 8 | Effects on pressure with $Re = 20$ for $n = 0.3, 1$ and 1.7 .

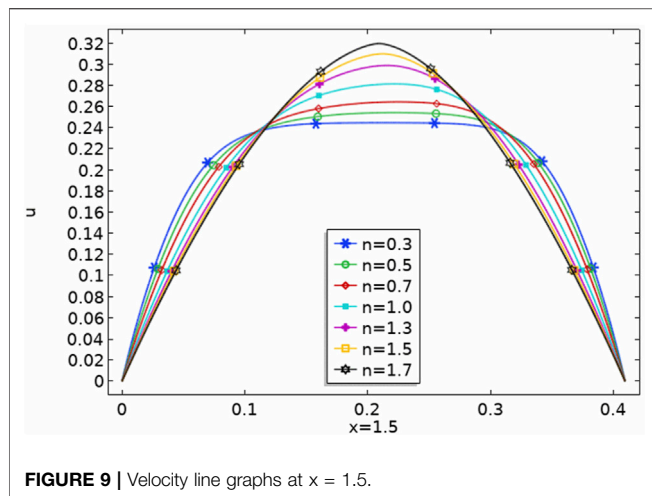


FIGURE 9 | Velocity line graphs at $x = 1.5$.

CONCLUDING REMARKS

The influence of shape and orientation of obstacles on hydrodynamic forces has been studied in the present work. A statistical analysis is also performed by computation on the correlation coefficient for all cases. Code validation is performed as a special case, and results show excellent agreement with the reference values of the drag and lift coefficients. The main findings are mentioned below:

- High-velocity magnitude is observed for the shear-thinning cases.
- Pressure dispersion from the stagnation point is also highly associated with the power-law index.
- A strong and positive correlation is observed between drag and lift when cylinders are taken separately.
- The case of a dual cylinder placed in a channel; an inverse association between drag and lift is observed at the semi-circular cylinder.

DATA AVAILABILITY STATEMENT

The raw data supporting the conclusions of this article will be made available by the authors, without undue reservation.

AUTHOR CONTRIBUTIONS

Conceptualization, RM, AHM, and IS; methodology, AM and IS; writing –original draft preparation, AHM and AM; supervision, RM and IS; writing –review and editing, NH and IK; Software, MT and NH; Validation, MT; Funding acquisition, MT, IS, NH, and IK, Formal analysis, NH. All authors have read and agreed to the published version of the manuscript.

REFERENCES

1. Tritton DJ. Experiments on the Flow Past a Circular cylinder at Low Reynolds Numbers. *J Fluid Mech* (1959) 6(4):547–67. doi:10.1017/s0022112059000829
2. Dennis SCR, Chang G-Z. Numerical Solutions for Steady Flow Past a Circular cylinder at Reynolds Numbers up to 100. *J Fluid Mech* (1970) 42(3):471–89. doi:10.1017/s0022112070001428
3. Fornberg B. A Numerical Study of Steady Viscous Flow Past a Circular cylinder. *J Fluid Mech* (1980) 98(4):819–55. doi:10.1017/s0022112080000419
4. Fornberg B. Steady Viscous Flow Past a Circular cylinder up to Reynolds Number 600. *J Comput Phys* (1985) 61(2):297–320. doi:10.1016/0021-9991(85)90089-0
5. Peregrine DH. A Note on the Steady high-Reynolds-number Flow about a Circular cylinder. *J Fluid Mech* (1985) 157:493–500. doi:10.1017/s0022112085002464
6. Cliff R, Grace JR, Weber ME. *Bubbles, Drops and Particles*. New York: Academic Press (1978).
7. Zdravkovich MM. *Flow Around Circular Cylinders: Volume 2: Applications*, Vol. 2. Oxford, United Kingdom: Oxford University Press (2003).
8. Kim T, Flynn MR. Numerical Simulation of Air Flow Around Multiple Objects Using the Discrete Vortex Method. *J Wind Eng Ind Aerodyn* (1995) 56(2–3): 213–34. doi:10.1016/0167-6105(94)00090-z
9. Bergstrom DJ, Wang J. Discrete Vortex Model of Flow over a Square cylinder. *J Wind Eng Ind Aerodynamics* (1997) 67-68:37–49. doi:10.1016/s0167-6105(97)00061-5
10. Taylor I, Vezza M. Prediction of Unsteady Flow Around Square and Rectangular Section Cylinders Using a Discrete Vortex Method. *J Wind Eng Ind Aerodyn* (1999) 82(1–3):247–69. doi:10.1016/s0167-6105(99)00038-0
11. Oertel H, Jr. Wakes behind blunt Bodies. *Annu Rev Fluid Mech* (1990) 22: 539–62. doi:10.1146/annurev.fl.22.010190.002543
12. Coutanceau M, Defaye J-R. Circular cylinder Wake Configurations: A Flow Visualization Survey. *Appl Mech Rev* (1991) 44:255–305. doi:10.1115/1.3119504
13. Norberg C. Fluctuating Lift on a Circular cylinder: Review and New Measurements. *J Fluids Structures* (2003) 17(1):57–96. doi:10.1016/s0889-9746(02)00099-3
14. Huang Y, Wu W, Zhang H. Numerical Study of Particle Dispersion in the Wake of Gas-Particle Flows Past a Circular cylinder Using Discrete Vortex Method. *Powder Tech* (2006) 162(1):73–81. doi:10.1016/j.powtec.2005.09.008
15. Luo K, Fan J, Li W, Cen K. Transient, Three-Dimensional Simulation of Particle Dispersion in Flows Around a Circular cylinder $Re=140-260$. *Fuel* (2009) 88(7):1294–301. doi:10.1016/j.fuel.2008.12.026
16. Dumouchel F, Lecordier JC, Paranthoën P. The Effective Reynolds Number of a Heated cylinder. *Int J Heat Mass Transfer* (1998) 41(12):1787–94. doi:10.1016/s0017-9310(97)00293-7
17. Berrone M, Garbero V, Massimo M. Numerical Simulation of Low-Reynolds Number Flows Past Rectangular Cylinders Based on Adaptive Finite Element and Finite Volume Methods. *Comput. Fluids* (2011) 40(7):14. doi:10.1016/j.compfluid.2010.08.014
18. Liu Z, Kopp GA. High-resolution Vortex Particle Simulations of Flows Around Rectangular Cylinders. *Comput Fluids* (2011) 40(1):2–11. doi:10.1016/j.compfluid.2010.07.011
19. Schewe G. Reynolds-number-effects in Flow Around a Rectangular cylinder with Aspect Ratio 1:5. *J Fluids Structures* (2013) 39:15–26. doi:10.1016/j.jfluidstructs.2013.02.013
20. Sivakumar P, Prakash Bharti R, Chhabra RP. Effect of Power-Law index on Critical Parameters for Power-Law Flow across an Unconfined Circular cylinder. *Chem Eng Sci* (2006) 61(18):6035–46. doi:10.1016/j.ces.2006.05.031
21. Kumar B, Mittal S. Effect of Blockage on Critical Parameters for Flow Past a Circular cylinder. *Int J Numer Meth Fluids* (2006) 50(8):987–1001. doi:10.1002/fld.1098
22. Rao PK, Sahu AK, Chhabra RP. Momentum and Heat Transfer from a Square cylinder in Power-Law Fluids. *Int J Heat Mass Transf* (2011) 54(1–3):390–403. doi:10.1016/j.ijheatmasstransfer.2010.09.032
23. Chandra A, Chhabra RP. Flow over and Forced Convection Heat Transfer in Newtonian Fluids from a Semi-circular cylinder. *Int J Heat Mass*

- Transf* (2011) 54(1–3):225–41. doi:10.1016/j.ijheatmasstransfer.2010.09.048
24. Faruquee Z, Ting DS-K, Fartaj A, Barron RM, Carriveau R. The Effects of axis Ratio on Laminar Fluid Flow Around an Elliptical cylinder. *Int J Heat Fluid Flow* (2007) 28(5):1178–89. doi:10.1016/j.ijheatfluidflow.2006.11.004
 25. Rao PK, Sahu AK, Chhabra RP. Flow of Newtonian and Power-Law Fluids Past an Elliptical cylinder: a Numerical Study. *Ind Eng Chem Res* (2010) 49(14):6649–61. doi:10.1021/ie100251w
 26. Kumar De A, Dalal A. Numerical Simulation of Unconfined Flow Past a Triangular cylinder. *Int J Numer Meth Fluids* (2006) 52(7):801–21. doi:10.1002/flid.1210
 27. Bhatti MM, Riaz A, Zhang L, Sait SM, Ellahi R. Biologically Inspired thermal Transport on the Rheology of Williamson Hydromagnetic Nanofluid Flow with Convection: an Entropy Analysis. *J Therm Anal Calorim* (2021) 144:2187–202. doi:10.1007/s10973-020-09876-5
 28. Bhatti MM, Zeeshan A, Bashir F, Sait SM, Ellahi R. Sinusoidal Motion of Small Particles through a Darcy-Brinkman-Forchheimer Microchannel Filled with Non-newtonian Fluid under Electro-Osmotic Forces. *J Taibah Uni Sci* (2021) 15(1):514–529. doi:10.1080/16583655.2021.1991734
 29. Cuahutenango-Barro B, Taneco-Hernández MA, Gómez-Aguilar JF. On the Solutions of Fractional-Time Wave Equation with Memory Effect Involving Operators with Regular Kernel. *Chaos, Solitons & Fractals* (2018) 115:283–99. doi:10.1016/j.chaos.2018.09.002
 30. El-Ajou A, Oqielat MN, Al-Zhour Z, Kumar S, Momani S. Solitary Solutions for Time-Fractional Nonlinear Dispersive PDEs in the Sense of Conformable Fractional Derivative. *Chaos* (2019) 29(9):093102. doi:10.1063/1.5100234
 31. Kumar S, Kumar A, Momani S, Aldhaifallah M, Nisar KS. Numerical Solutions of Nonlinear Fractional Model Arising in the Appearance of the Strip Patterns in Two-Dimensional Systems. *Adv Differ Equ* (2019) 2019(1):413. doi:10.1186/s13662-019-2334-7
 32. Sharma B, Kumar S, Cattani C, Baleanu D. Nonlinear Dynamics of Cattaneo–Christov Heat Flux Model for Third-Grade Power-Law Fluid. *J Comput Nonlinear Dyn* (2020) 15(1). doi:10.1115/1.4045406
 33. Santos TF, Santos CMS, Aquino MS, Ionesi D, Medeiros JI. Influence of Silane Coupling Agent on Shear Thickening Fluids (STF) for Personal protection. *J Mater Res Tech* (2019) 8(5):4032–9. doi:10.1016/j.jmrt.2019.07.013
 34. Othman MIA, Said S, Marin M. A Novel Model of Plane Waves Otwo-Temperature Fiber-Reinforced Thermoelastic Medium under the Effect of Gravity with Three-Phase-Lag Model. *Int J Numer Meth Heat Fluid Flow* (2019) 29. 359. doi:10.1108/hff-04-2019-0359
 35. Marin M, Othman MIA, Seadawy AR, Carstea C. A Domain of Influence in the Moore–Gibson–Thompson Theory of Dipolar Bodies. *J Taibah Uni Sci* (2020) 14:653. doi:10.1080/16583655.2020.1763664
 36. Mahmood R, Bilal S, Majeed AH, Khan I, Sherif E-SM. A Comparative Analysis of Flow Features of Newtonian and Power Law Material: A New Configuration. *J Mater Res Technol* (2019) 9(2):1978–1987. doi:10.1016/j.jmrt.2019.12.030
 37. Mahmood R, Bilal S, Majeed AH, Khan I, Nisar KS. CFD Analysis for Characterization of Non-linear Power Law Material in a Channel Driven Cavity with a Square cylinder by Measuring Variation in Drag and Lift Forces. *J Mater Res Tech* (2020) 9(3):3838–46. doi:10.1016/j.jmrt.2020.02.010
 38. Bilal S, Mahmood R, Majeed AH, Khan I, Nisar KS. Finite Element Method Visualization about Heat Transfer Analysis of Newtonian Material in Triangular Cavity with Square cylinder. *J Mater Res Tech* (2020) 9(3):4904–18. doi:10.1016/j.jmrt.2020.03.010
 39. Majeed AH, Jarad F, Mahmood R, Siddique I. Topological Characteristics of Obstacles and Nonlinear Rheological Fluid Flow in Presence of Insulated Fins: A Fluid Force Reduction Study. *Mathematical Problems in Engineering* (2021) 2021. 9199512. doi:10.1155/2021/9199512
 40. Majeed AH, Mahmood R, Abbasi WS, Usman K. Numerical Computation of MHD Thermal Flow of Cross Model over an Elliptic Cylinder: Reduction of Forces via Thickness Ratio. *Mathematical Problems in Engineering* (2021) 2021. 2550440. doi:10.1155/2021/2550440
 41. Mehmood A, Mahmood R, Majeed AH, Awan FJ. Flow of the Bingham Papanastasiou Regularized Material in a Channel in the Presence of Obstacles: Correlation between Hydrodynamic Forces and Spacing of Obstacles. *Modelling and Simulation in Engineeringub* (2021) 2021. 5583110. doi:10.1155/2021/5583110
 42. Ahmad H, Mahmood R, Hafeez MB, Majeed AH, Askar S, Shehzad H. Thermal Visualization of Ostwald-De Waele Liquid in Wavy Trapezoidal Cavity: Effect of Undulation and Amplitude. *Case Stud Therm Eng.* (2022) 29. 101698. doi:10.1016/j.csite.2021.101698
 43. Schäfer M, Turek S, Durst F, Krause E, Rannacher R. Benchmark Computations of Laminar Flow Around a cylinder In: EH Hirschel, editors *Flow Simulation with High-Performance Computers II*. Berlin/Heidelberg, Germany: Springer (1996). p. 547–66. doi:10.1007/978-3-322-89849-4_39

Conflict of Interest: The authors declare that the research was conducted in the absence of any commercial or financial relationships that could be construed as a potential conflict of interest.

Publisher’s Note: All claims expressed in this article are solely those of the authors and do not necessarily represent those of their affiliated organizations, or those of the publisher, the editors, and the reviewers. Any product that may be evaluated in this article, or claim that may be made by its manufacturer, is not guaranteed or endorsed by the publisher.

Copyright © 2022 Mahmood, Majeed, Tahir, Saddique, Hamadneh, Khan and Mehmood. This is an open-access article distributed under the terms of the Creative Commons Attribution License (CC BY). The use, distribution or reproduction in other forums is permitted, provided the original author(s) and the copyright owner(s) are credited and that the original publication in this journal is cited, in accordance with accepted academic practice. No use, distribution or reproduction is permitted which does not comply with these terms.